ELSEVIER

Coordination Chemistry Reviews 144 (1995)
39–68

COORDINATION CHEMISTRY REVIEWS

Zeolite-encapsulated and clay-intercalated metal porphyrin, phthalocyanine and Schiff-base complexes as models for biomimetic oxidation catalysts: an overview

Fethi Bedioui

Laboratoire d'Electrochimie et de Chimie Analytique (URA no. 216 du CNRS), Ecole Nationale Supérieure de Chimie de Paris, 11 rue Pierre et Marie Curie, 75231 Paris Cedex 05, France

Received 21 March 1994; in revised form 28 July 1994

Contents

Abstract

This paper reviews some important recent work on the design and characterization of zeolite-encapsulated and clay-intercalated metal–Schiff-base, –porphyrin and –phthalocyanine complexes. After an introduction to the chemistry of clays and zeolites, the incorporation

SSDI 0010-8545(94)08000-3

methods of these complexes within the mineral materials are discussed and an overview of their physicochemical characterization is reported. A large part of this paper is devoted to the reactivity of the zeolite- and clay-encapsulated complexes in biomimetic oxidation reactions.

Keywords: Clays; Zeolites; Biomimetic oxidation catalysts; Schiff bases; Porphyrins; Phthalocyanines

1. Introduction

Molecular engineering is now reaching highly elaborate levels of sophistication, and the analysis of the cooperative behavior of subunits within a controlled spatial assembly is a field undergoing a phase of explosive growth. Bioinorganic chemistry, which deals with a large variety of disciplines, is now profiting from the design of molecular systems and nanoscale machineries. In fact, bioinorganic structural motifs can potentially model metalloenzyme structures and functions in terms of steric effects imposed by the inorganic edifice. The aim of such modeling is to mimic natural properties and characteristics by focusing on a number of questions in order to elucidate fundamental aspects of reactivity and/or chemical mechanisms.

The desire to mimic enzymatic systems has prompted an extensive area of research into synthetic porphyrin, phthalocyanine and Schiff-base models of enzyme active sites, especially for monoxygenase enzymes of the cytochrome P-450 family [1–3]. Comparative studies of selectivity and stability in both the synthetic models (see some structures in Fig. 1) and natural systems, in the case of the biomimetic oxidation of hydrocarbons, led to the conclusion that selectivity arises from the steric effects imposed by the environment of the enzyme active site upon substrate approach [3–6], but also from specific binding at the active site. That is why this field of research has been the subject of intense efforts in order to mimic, in a first approach, the protein cavity of natural enzymes by designing synthetic superstructured porphyrin models with a controlled steric environment such as picnic-basket porphyrins, strapped porphyrins, etc. [7]. A similar conceptual approach has been developed during the last few years and is based on the replacement of the protein portion of natural enzymes by a size- and shape-selective framework of a mineral matrix such as clays and zeolites. This approach can be rationalized by imagining that the inorganic materials will provide the best arrangement for the catalytically active centres and will direct the substrate towards these centres [8–13]. Fig. 2 illustrates this concept. In this context, some of the recent published work that has involved zeolite-encapsulated and clay-intercalated metal complexes (porphyrins, phthalocyanines and Schiff bases) as biomimetic oxidation catalysts and oxygen carriers — so-called *inorganic enzymes* — is reviewed herein.

2. Introduction to clay chemistry

2.1. Smectites

Clays are colloidal layered hydrous aluminosilicates [14,15] and belong to the class of phylosilicates. The clay minerals known as smectites possess a combination

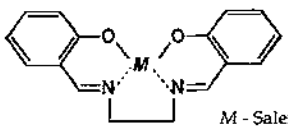

(a)

M - Salen

M = Co(II), Fe(III), Mn(III).

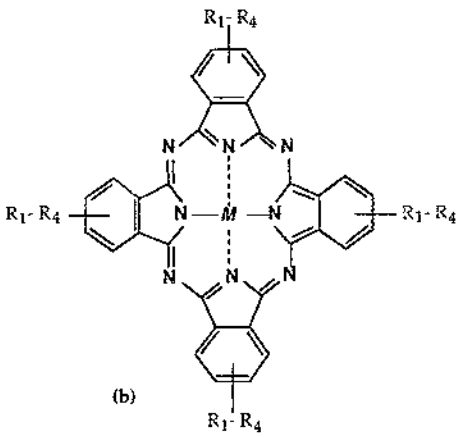

(b)

M -Pc : R_1- R_4 = H

M -TSPc R_1, R_2, R_4 = H

$R_3 = SO_3^-$

M = Co(II), Fe(II), Cu(II)

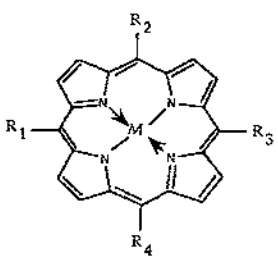

(c)

M -TPP : R_1- R_4 =

M -TSPP : R_1- R_4 =

M -TMPyP : R_1- R_4 =

M = Co(II), Fe(III), Mn(III).

Fig. 1. Structures of various synthetic models of cytochrome P-450: (a) metal–Schiff-base; (b) metallophthalocyanine; (c) metalloporphyrin.

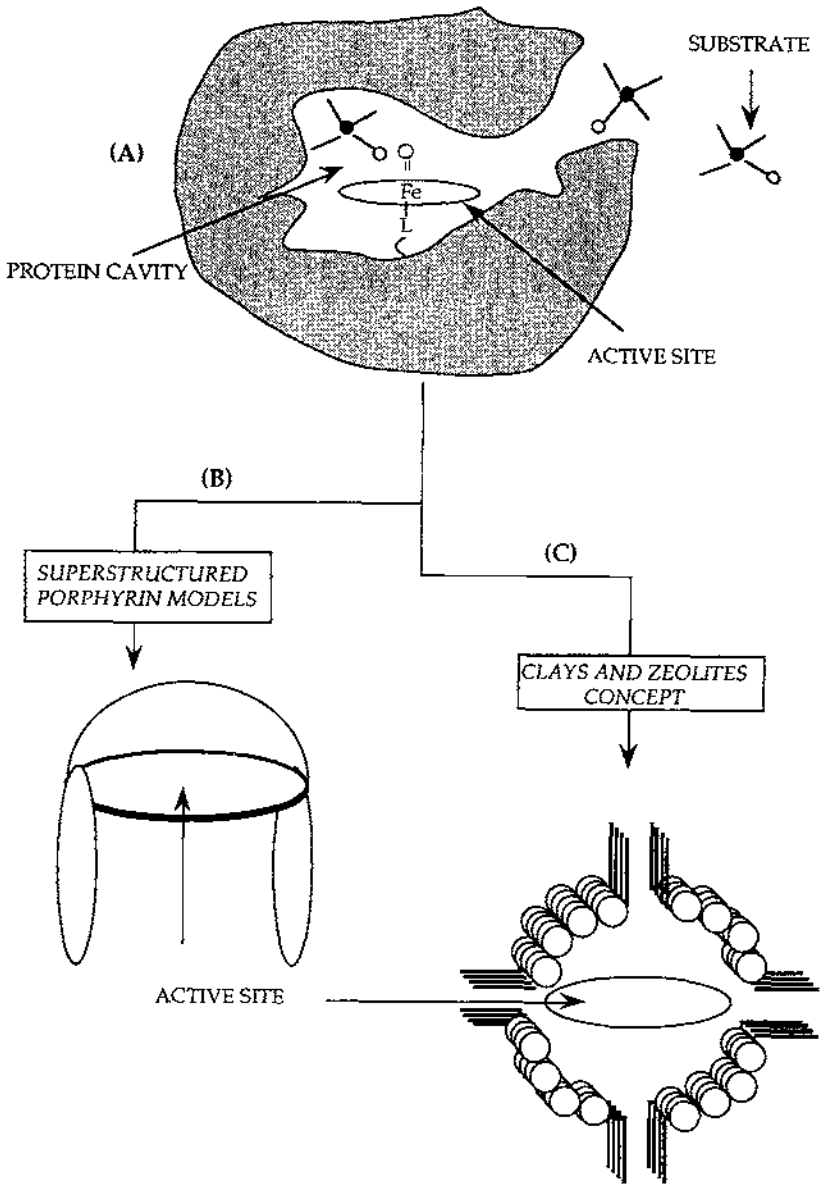

Fig. 2. Conceptual approaches for mimicking the protein portion of natural enzymes (A) (i.e. cytochrome P-450) by designing synthetic superstructured porphyrins (B) or using clay or zeolite mineral hosts for the enzyme active site (C).

of cation exchange, intercalation and swelling (or expanding) properties which makes them popular in host–guest chemistry. Fig. 3 schematically illustrates the oxygen framework of a smectite clay mineral such as montmorillonite (the most commonly used clay). The layers are assembled from sheets of SiO_4 tetrahedra and AlO_6

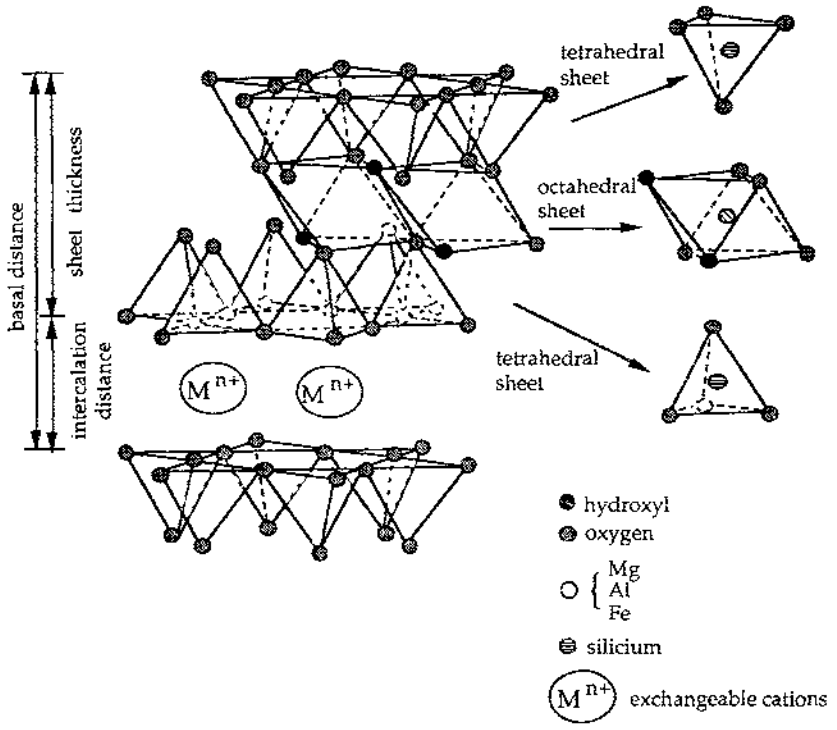

Fig. 3. Schematic structure of a smectite clay mineral, such as montmorillonite (adapted from Ref. [15]).

octahedra as an Al-octahedral sheet sandwiched between two Si-tetrahedral sheets with the oxygen atoms on the apices of the tetrahedra shared with the octahedra. In montmorillonite, the layer charge originates from the substitution of octahedral Al(III) by Mg(II). The positive charge deficiency is balanced by exchangeable cations (Na^-, K^+, etc.) which are distributed over both the interlayer and external surfaces of the clay. The clay layers are coupled through relatively weak dipolar and Van der Waals forces. The distance between the layers, or the basal distance (also called C-spacing) is revealed by X-ray diffraction and depends mainly upon the number of intercalated water and cation molecules within the interlamellar spaces. For dry Na^+- montmorillonite, the basal distance is about 12 Å and the layers collapse to a distance of 9 Å when the clay is heated to 500 °C. In hydrated montmorillonite, the introduction of water molecules within the interlayer region may provoke the enhancement of the C-spacing to as much as 20 to 50 Å. Finally, the cation exchange capacity of montmorillonite is typically 70–100 meq per 100 g.

2.2. Layered double hydroxides

Synthetic hydrotalcite-like materials, also called layered double hydroxides (denoted LDH) are Mg–Al compounds consisting of positively brucite-like layers $[Mg_6Al_2(OH)_{16}]^{2+}$ with exchangeable compensating anions, such as CO_3^{2-} in the

interlayer regions [16] (Fig. 4). Various anions can be intercalated into LDH structures by a variety of synthetic routes.

2.3. Pillared clays

Pillared clays are a relatively new class of lamellar solids recently reviewed by Pinnavaia [17,18]. They are prepared by exchanging the interlamellar ions in ordinary forms of smectite or LDH clays by bulky, thermally stable and robust ions which act as molecular pillars, keeping the layers separated in the absence of a swelling solvent. In the case of smectite clays, and as illustrated in Fig. 5, various types of large cations such as tetra-alkylammonium ions, bicyclic amine cations, metal complexes and polynuclear hydroxy metal cations can be used as pillaring agents. The nature of the ions and the host clays gives rise to various different physical and catalytic properties.

3. Introduction to zeolite chemistry

Zeolites have crystalline open framework structures constructed from SiO_4 and AlO_4 tetrahedra linked through oxygen bridges [19,20]. Each oxygen atom is shared by two silicon or aluminum atoms. The large variety of zeolite structure types is a consequence of the flexibility of the Al–O–Si linkage, which depends on the conditions of their hydrothermal synthesis. The tetrahedral coordination of Si–O and Al–O permits a variety of ringed structures containing 4, 5, 6, 10 or 12 Si or Al atoms. These rings are joined to form prisms and more complex cages, and the cages are joined to give three-, two- or one-dimensional frameworks (see some examples shown in Fig. 6). Because these structures contain uniformly sized pores and channels in the range of 4 to 13 Å, zeolites are able to recognize, discriminate and organize molecules with precisions that can be less than 1 Å.

For example, in the natural faujasite and synthetic zeolites X and Y, a supercage of 13 Å inner diameter is connected via 12 rings of 8 Å to four other cages in a

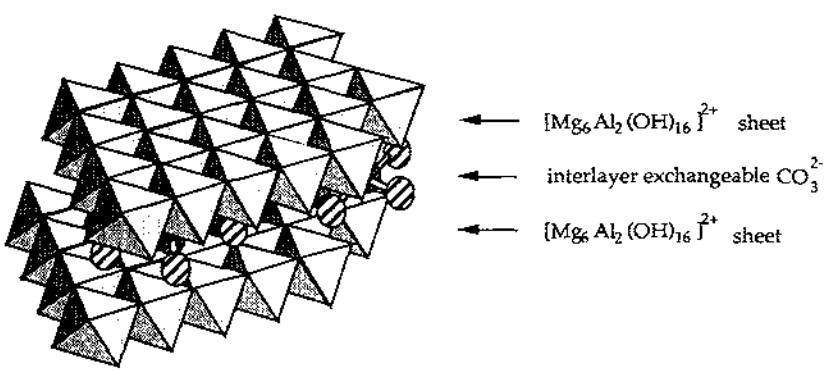

Fig. 4. Schematic structure of a hydrotalacite-like clay, such as layered double hydroxides.

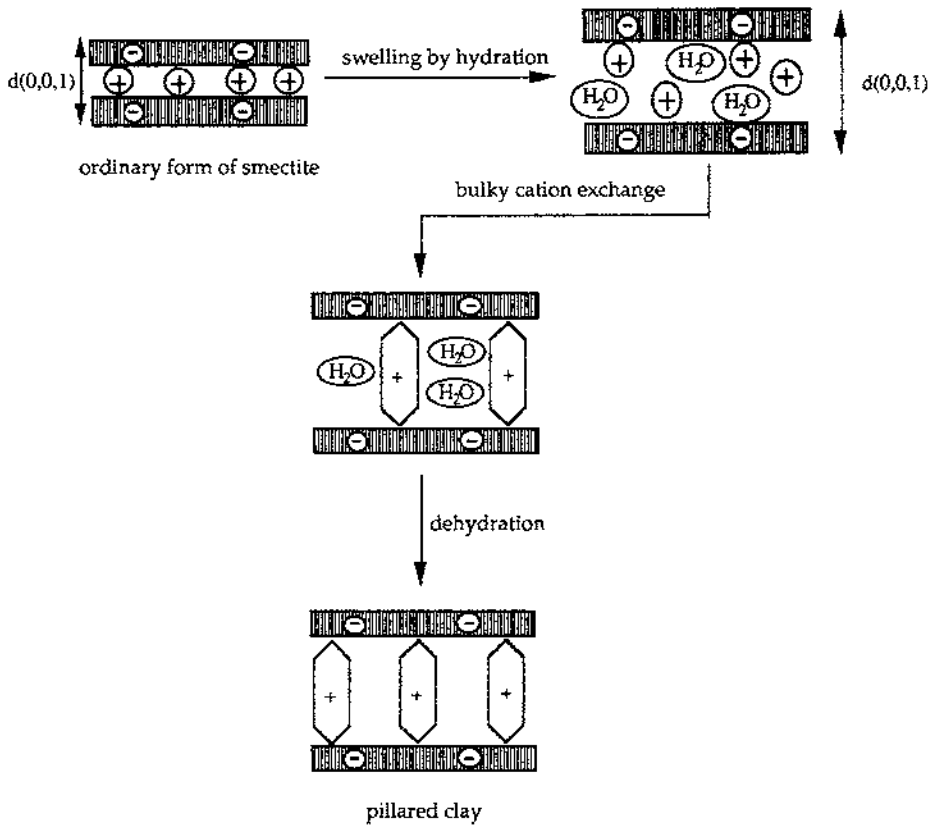

Fig. 5. General scheme for the synthesis of pillared clays (adapted from Ref. [18]).

tetrahedral arrangement. During their hydrothermal synthesis, the channel networks of zeolites are filled by water, which can be reversibly removed by heating. Typical composition of hydrated zeolite Y is $Na_{56}Al_{56}Si_{136}O_{384}\cdot 250H_2O$. The presence of Na^+ non-framework cations in zeolite structure is justified by the necessity of the balance of the negative charge of the framework generated by the formal -1 charge of the AlO_2 units. The existence of the exchangeable extra-framework cations provides to the zeolitic materials extra properties such as a fine-tuning of channel and pore dimensions and the possibility of inclusion of chemically interesting molecules.

In addition to the aluminosilicalite zeolites, several new classes of zeolite-like materials and synthetic molecular sieves has been reported in recent years. They were recently reviewed in the literature [21–25].

It appears from this introduction that the great interest in clays and zeolites arises from their well-known and defined structures. Clays have an adaptable sheet-like structure, while zeolites have rigid cages and channels with definite and uniform size. Thus, both of these materials may induce very interesting properties for designing new and selective supported catalysts.

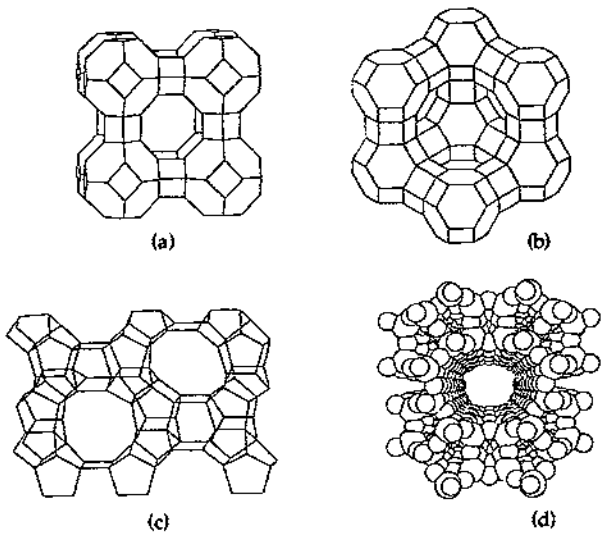

Fig. 6. Representative zeolite structures (adapted from Ref. [22]): (a) zeolites A; (b) zeolite Y, (c) zeolite ZSM-5 (the open framework is represented by sticks joining the Si or Al atoms. Oxygen bridge atoms, lying roughly at the mid-point of these atoms, are omitted for clarity); (d) zeolite mordenite (space-filling O atoms included).

4. Clay-intercalated metalloporphyrins and metallophthalocyanines

4.1. Preparation and physicochemical characterization

Few examples of clay intercalation of porphyrins and metallophthalocyanines are reported in the literature. The fixation process of the complexes is generally based on the ion-exchange properties of the mineral host.

4.1.1. Intercalation into montmorillonite

The pioneering studies on porphyrin fixation onto clays were developed in 1977 and were based on the physical adsorption of hemin, protoporphyrin and hematoporphyrin by montmorillonite in aqueous solutions buffered at pH 4 and 9 [26]. Cady and Pinnavaia [27] have reconsidered this approach, and they reported the reactions of meso-tetraphenylporphyrin free ligand ($TPPH_2$) with selected cations on the interlamellar surfaces of montmorillonite to give a small fraction of the neutral metallated porphyrin that remains physically adsorbed to the silicate layers. Bergaya and Van Damme [28] also reported the physical adsorption of various metal complexes of meso-tetraphenylporphyrin to montmorillonite. The porphyrin-clay solids were prepared by adding the air-dried clay to a chloroform solution of M(TPP) in a centrifugation cup. After the desired contact time, the suspension was centrifuged and the clay was washed several times with $CHCl_3$ until no more porphyrin could be extracted. It was shown from this study that the metalloporphyrins were relatively unstable in the clay environment, as evidenced by their demetallation. More recently,

Hu and Rusling [29] evaluated the behavior of surfactant-intercalated clay films to incorporate neutral molecules such as metallophthalocyanines (MPc). They have shown that clay–surfactant films containing metallophthalocyanines [29–31] have excellent stability. These materials were characterized by several techniques such as electrochemistry, electron absorption spectroscopy, scanning electron microscopy and X-ray powder diffraction.

The most common examples developed now are the binding of the tetracationic M(TMPyP) porphyrins (M = Co(II), Mn(III), Fe(III)) on montmorillonite clay [32–35]. These water-soluble metalloporphyrins are ion-exchanged into the interlayer spaces of montmorillonite from aqueous solution by soaking the mineral suspension for 1 to 2 h. Then the solid mineral is recovered by centrifugation and filtration, dried and crushed in a fine powder. It was also shown [33,35] that the Mn(TMPyP)-clay solid obtained did not release its porphyrin even after one week in acetonitrile. Moreover, it was very stable in more polar solvents like methanol or water. It is important to note that the porphyrin content in these materials varies from 1 to 8% by weight [35] (the total cation exchange capacity is 60% by weight for the tetracationic porphyrin). Fluorescence emission [32], electron absorption [32], UV–visible spectrophotometry [32–35] and X-ray powder diffraction [32–35] revealed the retention of the metal cation in the intercalated porphyrin. The UV–visible study of the supported porphyrins shows that none of them contain significant amounts of free-base porphyrin, indicating that demetallation never occurred during impregnation of Mn complexes [35].

As far as the Mn-porphyrins are concerned, the position of the Soret peak of Mn(TMPyP) varies from 453 to 471 nm, depending upon the conditions used. This indicates that the electronic and steric constraints caused by the support do not greatly modify the porphyrin structure in these supported complexes. The only exception comes from the Mn(TMPyP) porphyrin bound to montmorillonite (1% by weight), where the Soret peak is dramatically red-shifted to 496 nm. This was interpreted [35] as the result of a π interaction between the complex aromatic ring and the oxygen-atom planes of the aluminosilicates. In the case of clay-intercalated Mn(TMPyP) (5% by weight), the presence of two Soret peaks at 471 and 496 nm is indicative of the existence of two different kinds of Mn-porphyrins, a part of them being intercalated ($\lambda = 496$ nm) and strongly interacting with the layers. Mn(TMPyP)-clay porphyrins also display a small expansion of the basal spacings in X-ray diffraction spectra that are possibly due to the orientation of the interlamellar macrocycle parallel to the mineral sheets, as shown in Fig. 7. In fact one can imagine at least four different kinds of sites for complexes incorporated into clay solids, as is schematically shown in Fig. 8. The relative population of these different sites by a metalloporphyrin should probably depend upon the method of preparation of the complex–clay material [35].

The electrochemical characterizations of clay-intercalated Mn(TMPyP) porphyrin [36] provided additional evidence for the intercalation of the complexes between the interlayer sites. The results reported showed that the clay-intercalated porphyrins can be readily examined by electrochemical methods such as cyclic voltammetry. The Mn(III)/Mn(II) electroactivity is well defined in DMSO and H_2O solutions.

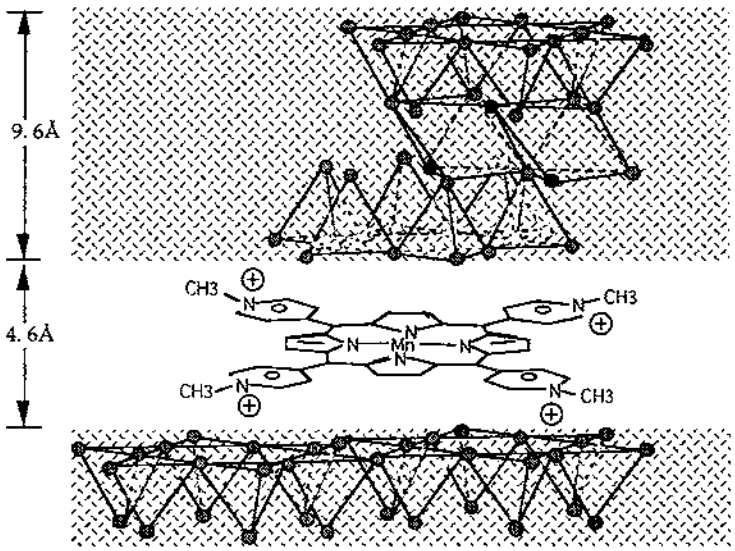

Fig. 7. Schematic illustration of the tetracationic Mn(III)-porphyrin, Mn(TMPyP), intercalated into the interlayer space of montmorillonite.

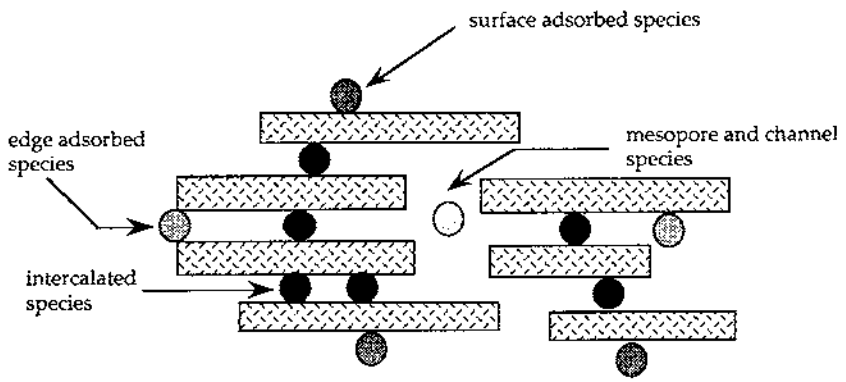

Fig. 8. Schematic representation of different sites for complexes incorporated into clay solids.

However, it was shown that, in acetonitrile media, the size of electrolyte cations affected the redox process response strongly.

New approaches to clay intercalation by metalloporphyrins are now under investigation. Carrado et al. [37] provided the first example of a hydrothermal crystallization of porphyrin-containing layer silicates by assuming that silicate structures can be determined, at least in part, by the shape of the intercalated molecule. Thus, the use of a large flat macrocycle like a porphyrin should normally help to induce silicate layer formation. The authors have succeeded in preparing porphyrin-containing smectite clays from synthesis gels by using TMPyP porphyrin and its metallo derivatives as organic templates. X-Ray powder diffraction data indicated that the

macrocycles are intercalated parallel between the clay layers. Microanalysis and UV–visible diffuse-reflectance measurements revealed that the porphyrins are incorporated intact. Recently, the same group [38] succeeded in intercalating phthalocyanines and metallophthalocyanines into the galleries of cationic smectites by in-situ crystallization of the clay layers under hydrothermal conditions. The complex contents correspond well to the expected exchange capacities of both the synthetic clays and their analogous ion-exchanged counterparts. The flat metallophthalocyanine molecules examined in that study were aligned parallel to the clay layers.

Another approach to porphyrin intercalation into clays consists of in-situ porphyrin synthesis within the mineral nanospaces. Onaka et al. [39,40] reported a recent example where meso-tetra-alkylporphyrins were synthesized in good yields from aliphatic aldehydes and pyrrole by using montmorillonite clay. The nanometer-size porous structures of the clay served as microreactors for the formation of the macrocyclic compounds. This approach, reconsidered by Laszlo and Luchetti [41] is generally aimed at making the porphyrin synthesis highly selective for a desired complex structure, without taking any other advantage from the physical intercalation of the complexes.

4.1.2. Intercalation into layered double hydroxides and other layered minerals

Tetra-anionic Mn(III) tetrasulfonated porphyrins [32] (MnTSPP) and Co(II) and Cu(II) phthalocyaninetetrasulfonate (MTSPc) [38,42,43] were successfully intercalated into LDH by ion exchange. In the case of the manganese porphyrins, the resulting LDH material contained 2.5 to 4.5% of Mn-complex which was not released by soaking the clay in dichloromethane, acetonitrile, methanol or water [35]. The intercalated porphyrins exhibited the expected UV–visible spectrophotometric behavior. The electrochemical characterization of these materials [44] showed that the redox behavior of the intercalated porphyrins can be readily examined by cyclic voltammetry. However, the slight solubility of Mn(TSPP) porphyrin in acetonitrile, dichloromethane and other solvents does not allow the comparison of its electrochemical behavior in the homogeneous phase with that in the supported phase.

Pèrez-Bernal et al. [42] reported, in the case of Co^{II}TSPc intercalated into LDH, that 92% of the clay exchange sites were balanced by the complex anions. The X-ray diffraction analysis of the clay material allowed the authors to conclude that the observed interlayer spacing of 23 Å was indicative of the intercalation of the complex with the plane of the phthalocyanine ring perpendicular, or nearly so, to the brucite sheets of the LDH host, as illustrated in Fig. 9. A similar "edge-on" orientation has also been previously reported for a non-metallated tetrasulfonated porphyrin anion intercalated into an LDH structure [45] in correlation with their host-layer charge densities. Recently, Carrado et al. [38] gave additional proof for the perpendicular arrangement of phthalocyanines to the brucite layers of LDH. The authors also showed that such an orientation of the macrocyclic complexes is effective whether they are incorporated directly (by in-situ crystallization of the synthetic clay layers) or via ion exchange. In the same way, Carrado et al. [38] provided a new and interesting method for the incorporation of porphyrins and phthalocyanines into clays via direct synthesis.

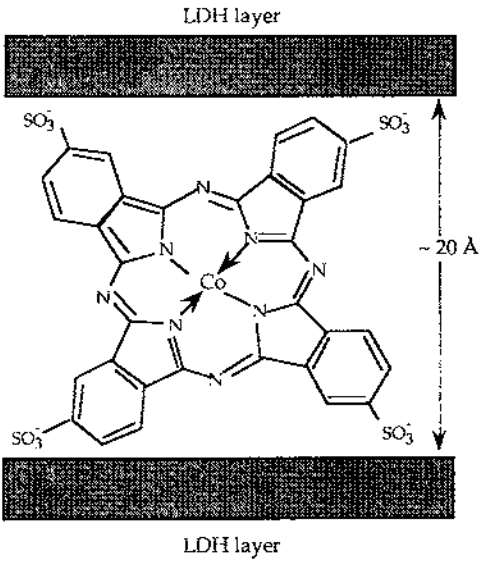

Fig. 9. Schematic illustration of the "edge-on" arrangement of Co(II) phthalocyaninetetrasulfonate intercalated in Mg–Al layered double-hydroxide clay (adapted from Ref. [42]).

Recently, Hudson et al. [46] reported that neutral cobalt phthalocyanine can be prepared in situ as a guest molecule in the layered host antimony hydrogen phosphate (denoted HSbP2). The 8% Co(II)-exchanged HSbP2 was heated with molten 1,2-dicyanobenzene at 230 °C for 1–4 h. The X-ray powder diffraction data indicated that there was only a small increase in the interlayer spacing on the formation of the cobalt phthalocyanine molecules, which therefore lie between the layers with the macrocyclic ring parallel to the phosphate sheets of the host. In addition, there was no evidence for delamination followed by reformation of the layers during the complex synthesis.

Binding of tetracationic porphyrins on layered antimony hydrogen phosphate [35] and zirconium hydrogen phosphate by ion exchange was also successfully reported by Kim et al. [47]. The authors discussed the preferred porphyrin orientations in terms of maximization of electrostatic and hydrogen-bonding interactions between the host and guest.

4.2. Biomimetic oxidation of hydrocarbons by clay-intercalated metalloporphyrins and phthalocyanines

Relatively few examples on biomimetic oxidation of hydrocarbons by clay-intercalated metalloporphyrins and/or phthalocyanines have been reported. However, they constitute an important contribution to the development of efficient chemical systems for hydrocarbon oxidation mimicking cytochrome P-450. The catalytic cycle of substrate oxidation by cytochrome P-450 [48], or by its synthetic metalloporphyrin models [49], involves the transfer of an oxygen atom, either

directly from oxygen atom donors such as PhIO, H_2O_2, ClO^-, ROOH, $KHSO_5$, ClO_2^-, RCO_3H and R_3NO, or from molecular oxygen after its reduction by two electrons to the porphyrinic catalytic site. This should lead to the formation of a high-valent metal-oxo species, formally a $[Fe(V)=O]^+$ or $[Mn(V)=O]^+$ complex as shown in Fig. 10. This species is highly reactive and is responsible for the oxidation of hydrocarbons to alcohols, ketones and epoxides.

Dixit and Srinivasan [50] reported the first study addressing the effect of a clay support on the catalytic epoxidation activity of a Mn(III)–Schiff-base complex. Their study has demonstrated that the radical decomposition of the hydroperoxide, used as oxygen atom donor, was suppressed on the clay-adsorbed catalyst. Thus, anchoring of the catalyst on the clay appeared beneficial when hydroperoxide is the oxidant, while no such advantage is realized with oxygen atom donors such as PhIO.

Barloy et al. [33] gave the first example of an efficient approach in the biomimetic activation of hydrocarbons by using Mn(TMPyP) porphyrin intercalated into montmorillonite and PhIO. They reported that the clay-intercalated Mn-porphyrin efficiently catalyzed the hydroxylation of heptane and pentane. The supported catalyst gave a better yield for heptane hydroxylation (60%) than the same porphyrin complex simply adsorbed on silica (40%) or used as an homogeneous catalyst (3%) [35]. Additionally, the catalyst intercalated into montmorillonite exhibited a marked shape selectivity in favor of small linear alkanes, when compared to a more bulky substrate [33–35]. This was shown by experiments on the competitive oxidation of adamantane (which is very reactive because of its tertiary CH bonds, but relatively bulky) and pentane (which is one of the least reactive substrates for the electrophilic metal-oxo species, but is less bulky than adamantane). The oxidation of a pentane/adamantane (2:1) mixture by PhIO in the presence of montmorillonite-intercalated Mn(TMPyP) led to an adamantanols/pentanols ratio of 77/33 which is clearly different from the (adamantanols + adamantanone)/(pentanols + pentanones) ratio of 97/3 obtained by the same catalyst in homogeneous phase or simply adsorbed on silica. This exclusive behavior of the clay-intercalated catalyst can be explained by the easier access of pentane, which is less bulky than adamantane, to the $[Mn(V)=O]^+$ active species intercalated in the interlayer spaces of the clay sheets.

We have recently reported a unique study involving the montmorillonite-

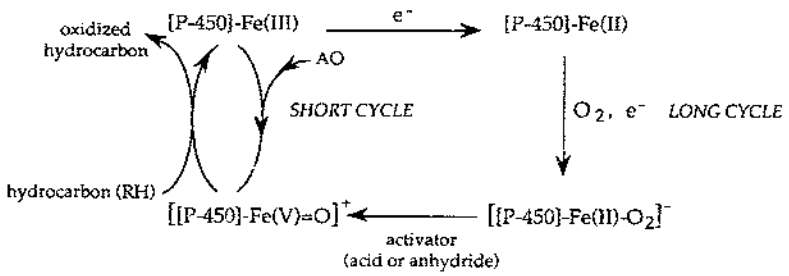

Fig. 10. Simplified catalytic cycle for the oxidation of hydrocarbons (RH) by molecular oxygen (long cycle) or by oxygen atom donnors AO (short cycle) and cytochrome P-450 (or its synthetic models) (adapted from Ref. [49]).

intercalated Mn(TMPyP) catalyst in the catalytic oxidation of hydrocarbons by molecular oxygen [51]. Our approach offered the double advantage of using O_2 and electrochemistry to generate the $[Mn(V)=O]^+$ active species. The supported catalyst was regenerated by controlled-potential electrolysis. In a typical experiment, the catalytic species was obtained by holding the potential of 50 mg of the montmorillonite-supported porphyrin (8% weight) in acetonitrile solution at $E=-0.3$ V(SCE) (SCE = saturated calomel electrode). The solution contained an axial base (0.125 mM of 1-methylimidazole), hydrocarbon (cyclo-octene, tetraline, cyclohexane or cyclooctane 0.01 M), benzoic anhydride (as the activator, 0.75 M) and supporting electrolyte (0.05 M tetrabutylammonium tetrafluoroborate + 0.05 M lithium tetrafluoroborate). Experiments were performed in two different kinds of electrochemical cells; (a) one-compartment cell with a soluble aluminium anode in which the solid montmorillonite supported porphyrin was in suspension, and (b) coulometric flow cell in which the solid montmorillonite-supported porphyrin was in a packed-bed compartment (see Fig. 11). All the experiments were performed under atmospheric oxygen pressure for 6 h at room temperature.

It was found that

(i) electrochemistry can be used in the biomimetic oxidation reactions by molecular oxygen catalyzed by clay-supported Mn(TMPyP),

(ii) the oxidation products were formed with a good efficiency of the supported catalyst, with up to 100 turnovers per hour,

(iii) the faradaic efficiency (expressed as the ratio of moles of oxidation products analyzed to electrochemical charge passed) and the catalytic activity (turnover) were greatly enhanced when the catalyst was supported on the clay. This exclusive enhancement in the catalyst performance is probably due to a preferred orientation of the supported catalyst for approach of the hydrocarbon to the presumed active manganese site. It also appeared that the nature of the coulometric procedure (suspension in a one-compartment cell or packed bed in a flow cell) had a significant influence on the faradaic efficiency of the supported catalyst. Additionally the clay-intercalated catalyst exhibited a marked shape- and regio-selectivity in favor of small hydrocarbons, such as cyclohexane, when compared to a more bulky substrate such as adamantane [53]. The results of the competitive oxidation experiments shown in Fig. 12 clearly indicate that the $[Mn(V)=O]^+$ active species intercalated in the interlayer spaces of the clay sheets can be easily formed electrochemically. This also provides additional evidence for the electrochemical accessibility of the interlamellar porphyrins.

Barloy et al. [35] also reported that supported Mn-porphyrins on layered double hydroxides and antimony hydrogen phosphate were good catalysts for cyclo-octene epoxidation and alkane hydroxydation by PhIO. The use of an LDH host for the intercalation of Co(II)-phthalocyanine oxidation catalysts was reported by Pinnavaia and co-workers [42,43]. The intercalated complex was used for the auto-oxidation of aqueous 1-decanethiol [42] and 2,6-di-ter-butylphenol [43] by molecular oxygen. In both cases, the LDH-intercalated catalyst was more active than the homogeneous one under equivalent reaction conditions. More importantly, the homogeneous catalyst was completely deactivated within 25 to 150 turnovers, whereas no loss in

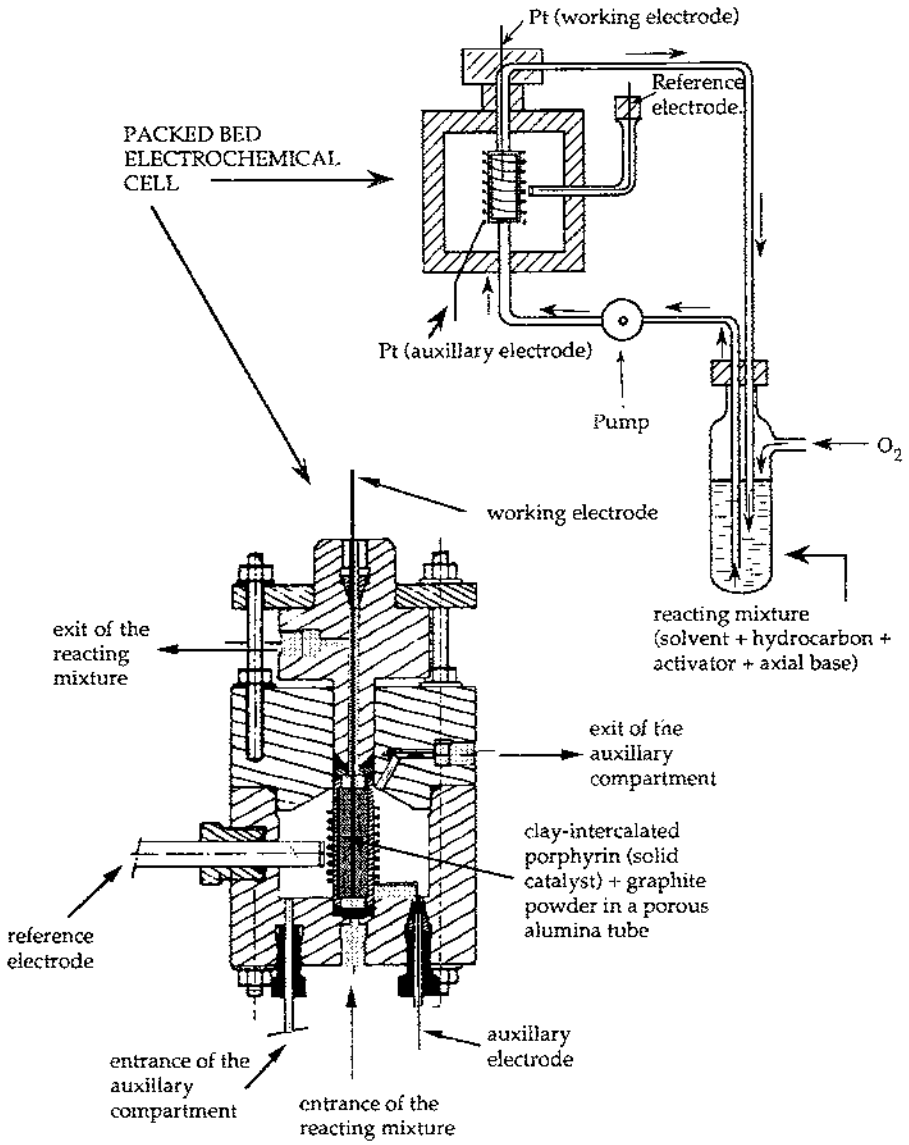

Fig. 11. Schematic illustration of the packed-bed electrochemical cell (adapted from Ref. [52]).

activity was observed for the intercalated catalyst even after more than 3200 turnovers. Thus, layered double-hydroxide intercalation compounds appeared to be exceptionally efficient support-mineral materials for improving the stability of biomimetic metallo macrocyclic catalysts. The increase in the catalyst stability may be explained in terms of site isolation of the active species which prevents the deactivation of the complex via a binuclear pathway (dimerization, etc.).

Analysis of the available data [33–35,53] shows clearly that the clay-intercalation

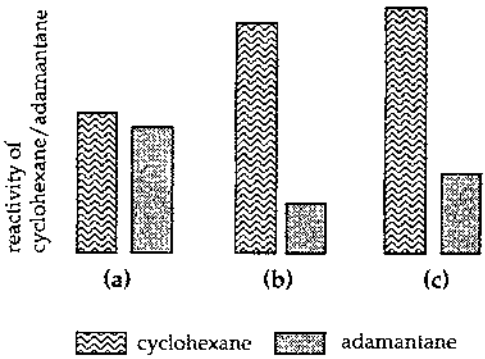

Fig. 12. Bar-graph representation of substrate selectivities in cyclohexane and adamantane competitive oxidation by molecular oxygen electrocatalyzed by (a) Mn(TMPyP) dissolved in homogeneous solution; (b) Mn(TMPyP) intercalated into montmorillonite; (c) Mn(TMPyP) intercalated into montmorillonite using Zn powder as reducing agent (adapted from Ref. [53]).

of the porphyrin catalysts is efficient. It also leads to the expected size and shape selectivities despite the non-rigid structure of the sheet-like mineral hosts.

5. Zeolite-encapsulated metal–Schiff-base and –phthalocyanine complexes

Owing to their large size (10 to 14 Å), metal–Schiff-base, –porphyrin and –phthalocyanine complexes cannot be fixed within the porous structures of zeolites by anion exchange process. In fact, the largest pores and cavities apertures are of 8 Å diameter in the case of Y-type faujasite. We reported in 1985 the first example of zeolite-supported M(TMPyP) porphyrins [54] and their use in electrocatalysis [55]. The macrocyclic porphyrin was simply adsorbed on the external surface of the zeolite grains, which did not provide the shape- and size-selectivity inherent in the host support. That is why, recently, the encapsulation or physical entrapment of coordination compounds within the cages of zeolites has attracted much interest. Thus, a large variety of metal complexes have been encapsulated in a range of different zeolite hosts, resulting in new composite materials with numerous applications. The so-called "ship-in-a-bottle" zeolite-based catalysts such as metal–Schiff-base, –porphyrin and –phthalocyanine complexes have been the subject of considerable intense research [8–10,13,56–91].

5.1. Zeolite-encapsulation methods

There have been basically three approaches to the preparation of these "ship-in-a-bottle" chelate complexes, namely the *flexible ligand* method, the *template synthesis* method and the *zeolite synthesis* method.

In the first approach, a flexible ligand must be able to diffuse freely through the zeolite pores, but upon complexation with a previously exchanged metal ion the complex becomes too large and rigid to the escape the cages. This approach is well

adapted for encapsulation of metal–Salen complexes (Salen = *N*,*N*′-bis (salicylaldehyde)ethylenediimine), since the Salen ligand offers the desired flexibility. Thus, a large variety of cobalt [56], manganese [57], iron [58], rhodium [59] and palladium [60] Salen complexes was prepared according to this method within the Y-faujasite supercages. In a typical experiment, the appropriate metal cation was placed into the Y-type zeolite cages via ion exchange. Then, approximately 2.0 g of previously exchanged Y/metal zeolite was combined with 2.0 g of freshly recrystallized Salen and heated to 150 °C. Upon fusion of the Salen ligand the mass was stirred frequently over 2–4 h. The mixture was then allowed to solidify and was crushed to a fine powder. This powder was extracted with successive portions of acetone, acetonitrile, dichloromethane and acetone for more than 24 h each in order to remove the unreacted Salen ligand and the surface-adsorbed complexes.

The template synthesis method is exemplified by the preparation of intrazeolite metallophthalocyanines [8,9,13,61–89]. This approach requires four dicyanobenzenes to diffuse into the zeolite matrix where they can cyclize around a resident metal ion (fixed by ion exchange) to form the tetradentate macrocycle which is too large to exit. In a typical experiment, approximately 1.0 g of the desired metal-exchanged zeolite (Co^{II}/Y, Fe^{II}/Y or Cu^{II}/Y) was activated at 150 °C under vacuum of 10^{-3} Torr for 2 h then cooled to room temperature. An excess of dicyanobenzene was introduced and the ampoule was again evacuated to 10^{-3} Torr, held at that pressure for 2 h and sealed. The finely powdered contents were thoroughly mixed and placed horizontally in a tube furnace and heated at 300 °C for 24 h. After reaction, the contents were pulverized, transferred to a Soxhlet thimble and extracted with successive portions of acetone, pyridine and acetonitrile for 24 h each to remove surface-adsorbed complexes. Synthesis of intrazeolite hexadecahalophthalocyanines ($MPcX_{16}$) according to this method, using tetrahalophthalonitriles as starting agent for the formation of the macrocycle, has also been reported [86–88].

The use of substituted dicyanobenzenes to form substituted phthalocyanines was also reported [78,89] but it was shown for tetranitrophthalocyanines that their insertion in the zeolite cages is doubtful, and that they are located mostly on the external surface [89]. In the case of FePc, iron(II)-exchanged NaY as well as adsorbed ferrocene or iron pentacarbonyl in NaY have been shown to be suitable starting materials [65,70,71,74,75,83,87]. Zeolite-impregnated iron pentacarbonyls are decomposed under thermal conditions, and the metal clusters formed react with dicyanobenzenes to give MPc with simultaneous oxidation of the metal [83]. The major disadvantage of this method is the formation of iron clusters. The use of adsorbed ferrocene as starting material was also successfully described by Parton et al. [74], who claimed that there was almost no residual iron. These authors extended the use of adsorbed metallocenes to molecular sieves without cation exchange capacity, such as VPI-5 [74]. Indeed, with ferrocene, FePc complexes were successfully prepared inside the molecular sieve. However, the presence of uncomplexed metal ion and free ligand inside the zeolite obtained in the template approach might be expected to complicate characterization and reactivity studies.

The most recent method for encapsulating metal complexes in zeolites, referred to as the zeolite synthesis method, involves the addition of the metal complex (especially metallophthalocyanine), possibly in a template role, during the crystallization of the

zeolite host [87,88,90]. This method of encapsulation offers several advantages over template synthesis, including mild preparation conditions and well-defined intrazeolite metal complexes. It was claimed for the neutral metallophthalocyanines that aggregation of the complexes in the aqueous synthesis medium can be overcome by careful design of the zeolite synthesis procedure [90]. Fig. 13 summarizes the different strategies and routes for the zeolite encapsulation of the complexes cited.

Finally, Nakamura et al. [91] and Chan and Wilson [68] reported the unique examples of Y-zeolite-encapsulated metalloporphyrins (iron and manganese tetramethyl- and tetraphenylporphyrins) by using the template synthesis method. However, no convincing data ensured the intrazeolite formation of the complexes.

5.2. Characterization of the zeolite-encapsulated complexes

5.2.1. Physicochemical studies

Complete characterization of the encapsulated complexes is mandatory in order to ensure the feasibility of the intrazeolite synthesis. Indeed, in the synthesis of well-

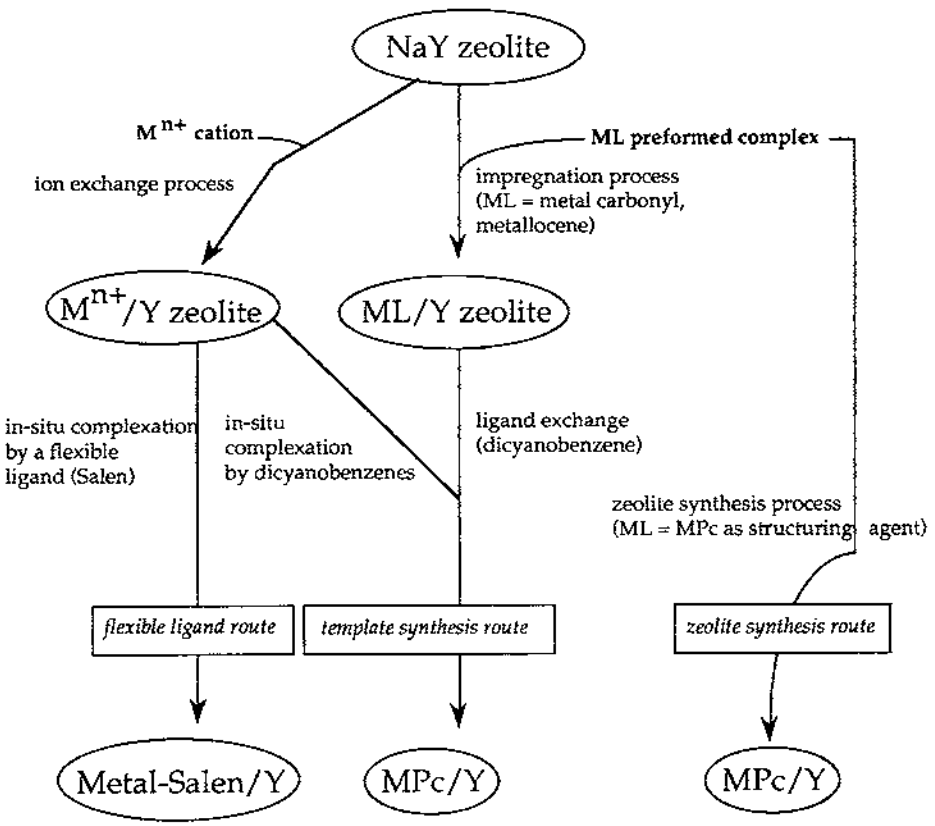

Fig. 13. Different strategies and routes for the zeolite-encapsulation processes (adapted from Ref. [13]).

defined macrocycles in the restricted space of pores, channels and cavities, many questions must be considered, such as:

(i) does the organic ligand form the desired complex?
(ii) in what yield is the desired complex obtained?
(iii) how deep inside the zeolite structure does the desired compound sit?
(iv) does the in-situ synthesis of the desired complex preserve the pore structure of the zeolite host?

In order to give a clear answer to each question, several techniques must be used in conjunction. Pàes-Mozo et al. [85] recently reported a handsome study dealing with the different characterization techniques usable in all the steps of the synthesis and purification procedures of a cobalt phthalocyanine encapsulated in Y zeolite.

The intrazeolite encapsulation of the metal complexes within the host supercages is usually characterized by a battery of techniques and procedures that may involve elemental analysis, Fourier transform infrared spectroscopy, surface analysis, thermogravimetric analysis, differential thermal analysis, X-ray diffraction, conventional transmission and high-resolution electron microscopy and electrochemistry. Chemical analysis was generally used in order to obtain information on the bulk composition of the chemically modified zeolites and to quantify their degree of exchange. X-Ray powder diffraction permits one to ensure that the zeolite host crystallinity remains after its chemical modification, while the size and shape of the solid particles may be studied by conventional transmission electron microscopy. Analysis down to the nanoscale of the individual unit cells may be performed by high-resolution electron microscopy. This technique may give evidence for the formation of complexes on or inside the zeolite crystallites and for any modification of the framework of the zeolite. The formation of the macrocyclic complexes was usually established by IR and UV–visible spectroscopic measurements and confirmed by additional studies of the modified zeolite by thermogravimetric and differential thermal analysis. Finally, X-ray photoelectron spectroscopy and Mössbauer spectroscopy may be very helpful for the determination of the exact location of the metal complexes within the cavities of the zeolite, as well as the nature of the encapsulated metal environment.

Recently, it was shown that the use of new mathematical and computerized tools such as molecular graphics analysis [10] may provide fruitful information on the zeolite-encapsulated complexes. Thus, it was shown in the case of Y-zeolite-encapsulated iron-phthalocyanine [74] that FePc was located in the faujasite structure with the centre of the molecule at the centre of the supercage, the bridging N atoms being oriented to the four-rings of the cubo-octahedra. To avoid overlap between the molecule and the zeolite structure, the planarity of the complex had to be disturbed, since the dimension of the phthalocyanine ligand (~ 14 Å) exceeds the effective diameter of the NaY or X supercage (~ 12 Å). This should result in a distortion of the macrocycle, which has been calculated to be a minimum of 37.3° from planarity [74,87], as shown in Fig. 14.

5.2.2. Electrochemical studies

Electrochemical techniques such as cyclic voltammetry are a simple, low-cost characterization method uniquely suited to provide information on the oxidation

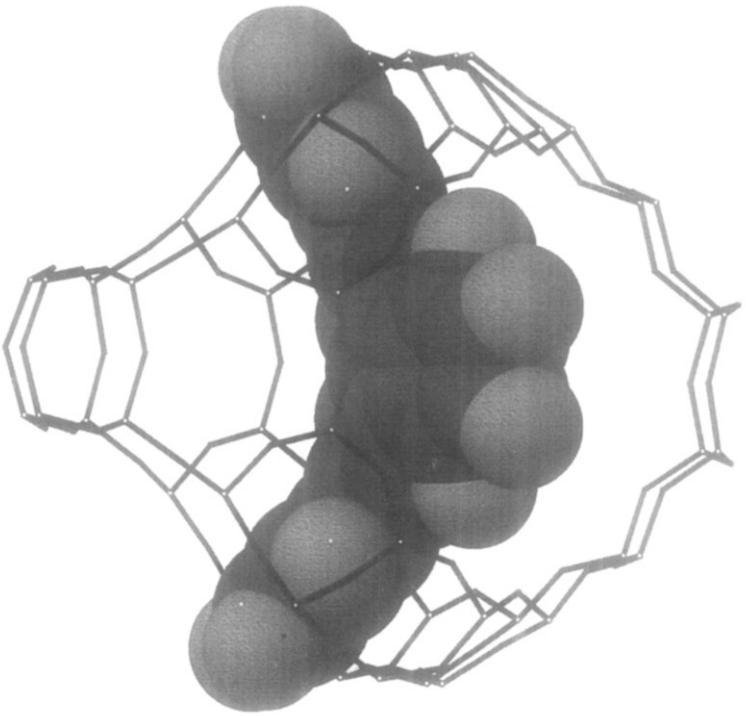

Fig. 14. Representation of minimized metallophthalocyanine complex encapsulated in a Y-faujasite-type supercage (calculated using CAChe molecular modeling [87]).

state and redox chemistry of the active metal atom and the ligand. Even subtle structural features may be elucidated through differences in potential shifts between two different complex structures. Thus, zeolite-modified electrodes and electrode-modified zeolites have been extensively used in the last decade and directed toward the design of electrocatalytic surfaces, as described in recent reviews [23,92–94]. However, in spite of the many advantages, little electrochemical characterization of the "ship-in-a-bottle" encapsulated macrocyclic complexes has been reported in the literature [58,86–88,95–98].

In the general case, two mechanisms suggested by Shaw et al. [99] for the electron transfer processes occurring at zeolite-modified electrodes can be considered:

$$E^{m+}_{(z)} + mC^{+}_{(s)} \Leftrightarrow E^{m+}_{(s)} + mC^{+}_{(z)}$$

$$E^{m+}_{(s)} + ne^{-} \rightarrow E^{(m-n)+}_{(s)} \quad (1)$$

$$E^{m+}_{(z)} ne^{-} + nC^{+}_{(s)} \rightarrow E^{(m-n)}_{(z)} + nC^{+}_{(z)} \quad (2)$$

where $E^{m}+$ is the electroactive species, (z) indicates the zeolite matrix, (s) indicates the solution and C^{+} is the electrolyte cation.

Mechanism (1) occurs only with small electroactive species, such as fixed within the zeolite by ion exchange, and which can move freely within the pore system. Thus,

the electron transfer takes place after the electroactive species is exchanged out of the zeolite by the electrolyte cations. Mechanism (2) involves physically entrapped electroactive species that undergo electron transfer within the zeolite cavities, such as zeolite-encapsulated complexes. Thus, it appears that in both mechanisms (1) and (2) the nature of the electrolyte cation should have a great influence on the electroactivity of the zeolite-modified electrodes.

Evidence for mechanism (1) has been reported for electroactive cations exchanged in different types of zeolites [92,93,98]. However mechanism (2) was not rejected in these studies. In the case of the zeolite-encapsulated "ship-in-a-bottle" complexes, our previously reported results [58,86–88,95–98] indicated that the electroactivity of the intrazeolite species can be readily examined by using pressed powder-composite graphite electrodes [54], as illustrated in Fig. 15. The electron transfer should occur primarily according to mechanism (2). Nevertheless, the electroactivity of these metal-complex-modified zeolites remains low, and this raises a serious debate on the origin of the observed electrochemical responses. However, we recently demonstrated further the possibility of electrochemical characterization of physically entrapped metal complexes inside the zeolite cavities by using the pressed powder-composite electrodes: we have shown [97] by cyclic voltammetry that Ni^0(bpy) encapsulated within Y-type zeolites can be selectivity implicated in electroassisted catalytic reduction of organic halides. Indeed, the encapsulated complexes show catalytic activity towards benzyl chloride, as evidenced by scanning the electrode potential through

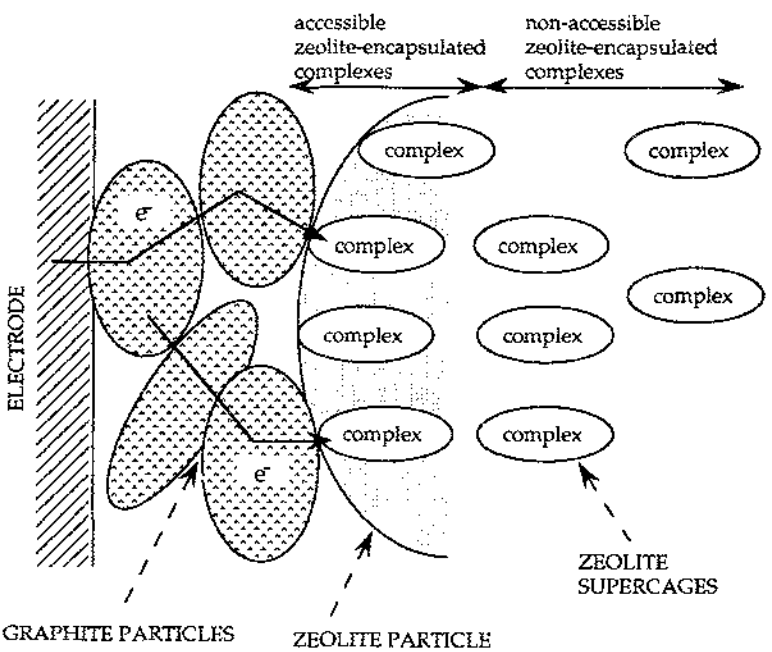

Fig. 15. Schematic illustration of the electron transfer reaction within a pressed graphite powder-composite electrode containing a zeolite-encapsulated complex.

the Ni(II)/Ni(0) redox process, while the large triphenylmethyl bromide molecule is unreactive. This shape selectivity corroborates the fact that the electrochemical response observed with the zeolite-encapsulated complexes reflects the activity of intrazeolite species. Thus, it seems that the zeolite framework serves as a relay between host species. (The concept of the zeolite as a solid electrolyte is an established one [100]).

New strategies are now being developed to improve the electrochemical accessibility of the encaged complexes by:

(i) using a new approach based on the vectorial electron transport from a bulky redox mediator on the surface of zeolite particles to the encapsulated complex in the bulk of the zeolite [98],

(ii) structuring nanometer-sized silver metallic particles on the zeolite surface and within the zeolitic cages to enhance the population of accessible encapsulated complexes [101].

Fig. 16 shows the cyclic voltammogram of the Fe^{III}Salen-encapsulated complex into Y-type faujasite (curve A), in DMSO + 0.1 M $LiClO_4$ solution [98]. This voltammogram exhibits a well-defined couple of peaks that can be attributed to the Fe^{III}/Fe^{II}Salen redox process of the intrazeolite complex. Curve B in Fig. 16 shows the cyclic voltammogram of zeolite Y modified by adsorption of Fe^{III}Salen complex on the external surface by ion exchange. By comparing curve A to curve B, it appears that the electrochemical response obtained from the only extrazeolite species is much lower than the one obtained from the "ship-in-a-bottle" complexes. This supports the contention that the surface concentration in the case of the zeolite-encapsulated complexes is extremely low and cannot possibly provide all the observed electroactivity.

Table 1 summarizes the reported results on the electrochemistry of the zeolite-encapsulated metal–Salen complexes [58,86,96]. It is important to note from these

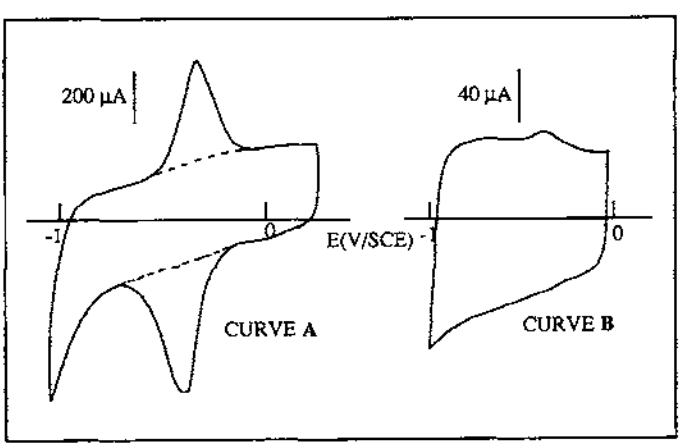

Fig. 16. Cyclic voltammogram of a pressed graphite powder-composite electrode containing (curve A) Y-zeolite-encapsulated Fe^{III}Salen and (curve B) Y-zeolite surface-adsorbed Fe^{III}Salen in DMSO + 0.1 M $LiClO_4$ solution (potential sweep rate = 10 mV s^{-1}) (adapted from Refs. [98,101]).

Table 1
Summary of redox potential values (E) for M^{III}/M^{II} redox processes determined for Y-zeolite-encapsulated metal-salen complexes and homogeneous solution of dissolved complexes in specific solvents

	Y-zeolite-encapsulated complex	Dissolved complex	Reference
Co^{II}Salen in DMSO + 0.1 M Bu_4NBF_4	$E_{eq1} = -80$ mV (SCE) $E_{eq2} = -800$ mV (SCE)	$E_{eq} = -20$ mV (SCE)	[96]
Fe^{III}Salen in CH_3CN + 0.1 M Bu_4NBF_4	$E_{eq1} = -350$ mV (SCE) $E_{eq2} = -800$ mV (SCE)	$E_{eq} = -320$ mV (SCE)	[58]
Fe^{III}Salen in CH_3CN + 0.1 M $LiBF_4$	$E_{eq} = -350$ mV (SCE)	$E_{eq} = -320$ mV (SCE)	[101]
Fe^{III}Salen in DMSO + 0.1 M Bu_4NBF_4	$E_{eq} = -350$ mV (SCE)	$E_{eq} = -300$ mV (SCE)	[58]
Mn^{III}Salen in CH_3CN + 0.1 M Bu_4NBF_4	$E_{eq} = -200$ mV (SCE)	$E_{eq} = -200$ mV (SCE)	[58]
Ru^{III}Salen in DMSO + 0.1 M Bu_4NBF_4	$E_{eq} = -380$ mV (SCE)	$E_{eq} = -380$ mV (SCE)	[86]

[a] Two redox processes are observed (see text).

results that Mn^{III}Salen and Ru^{III}Salen complexes show electrochemical behavior which is very similar to that of the dissolved complexes in solution. However, in the case of zeolite-encapsulated Co^{II}Salen and Fe^{III}Salen, these results suggest the existence of two M^{III}/M^{II} redox processes that can be related to the existence of two kinds of metal–Salen structures [58,96]: planar or non-planar tetradentate structures and bidentate structures involving coordination of Co^{II} by Salen in unusual ways. The observation of these structures seems to be dependent on the nature of both the solvent and the supporting electrolyte. In spite of the considerable uncertainty about the cobalt coordination geometry, these results show that the zeolite may be involved in the coordination of the metal ion. It is now well accepted that zeolite-encapsulation synthesis yields a mixture of coordinative environments. In the case of Mn^{III}Salen encapsulated complex, the voltammetric measurements show that the encaged complex reacts with dissolved O_2 in the presence of 1-methylimidazole [58], which presents new possibilities for using these materials in electrocatalytic oxidations. Finally, our reported results on the electrochemistry of zeolite-encapsulated perhalogenated phthalocyanines [88,98] revealed reversible M^{II}/M^{I} redox processes for the intrazeolite complexes that are difficult to observe in solution. The well-defined redox behavior of the inclusion compounds seems to be a consequence of their site isolation within the zeolite matrix, while the simple adsorption of the molecules on the electrode surface or on any other mineral support does not prevent aggregate formation.

5.3. Biomimetic oxidation of hydrocarbons by zeolite-encapsulated metallophthalocyanine and Salen complexes

There was early interest in using zeolite-encapsulated complexes as oxygen carriers mimicking haemoglobin, the oxygen-carrying iron porphyrin protein of blood [56,102,103]. The use of Y-zeolite-encapsulated Co^{II}Salen [56] has shown clearly that the entrapped complex binds oxygen reversibly and can separate oxygen from nitrogen in dry air. The zeolite framework, like an enfolding protein, prevents the complexes from dimerizing and degrading. The zeolite-encapsulated complexes are therefore more efficient reversible oxygen carriers than the homogeneous dissolved complexes which degrade in solution.

Herron et al. [66] reported the first example of zeolite-encapsulated iron phthalocyanine catalysts in hydrocarbon biomimetic oxidations in conjunction with iodosobenzene oxidizing agent. The zeolite-entrapped catalyst did, however, produce oxidized products in an identical homogeneous reaction procedure, but with some marked differences. Most significant was the increased turnover based on iron with the lower loading of FePc zeolites [8]. This result was interpreted as a result of the very effective site isolation within the cages, which prevents any bimolecular pathways to phthalocyanine catalyst destruction [57,66,67,74]. However, the catalytic oxidation reaction appeared to stop because the pore system of zeolite becomes clogged with reaction products, thus preventing further access of reagents and substrate to the active sites.

Another notable feature of the zeolite-encapsulated complex oxidations

[8,57,60,66,67,74] was their high size and shape selectivities. For example, in the case of Y-zeolite-encapsulated FePc, the expected substrate selectivity of the zeolite catalyst was shown in a competitive oxidation of cyclohexane and cyclododecane [66]. The zeolite-entrapped complexes showed a clear preference for oxidation of the smaller of the two substrates. Such selectivity presumably arises from the molecular sieving action of the zeolite support. In the oxidation of *n*-octane [66,74], regioselectivity was also apparent. A small but reproducible change in selectivity for oxidation away from the 4-position and towards the 2-position of octane was observed. This shift towards oxidation nearer the ends of the long axis of the molecule was also observed with methylcyclohexane. It was interpreted [8,66] as an orienting influence of the zeolite framework upon the substrate as it approaches the iron–oxo active site. Stereoselectivity was also observed with the zeolite-entrapped complexes [66,74] and was interpreted as a consequence of the substrate/catalyst relative orientation imposed by the zeolite. Fig. 17 illustrates the schematic representations of substrate, regio- and stereoselectivities in zeolite cages.

In a similar development of the biomimetic approach, Tolman and Herron [9,67] have described an efficient zeolite oxidation system which does not use metal complexes. They used a catalyst comprising Pd(0) and Fe(II) in an A-type zeolite with an oxygen–hydrogen mixture in selective oxidation of hydrocarbons. The palladium component catalyzed the formation of hydrogen peroxide, which then oxidized the hydrocarbon (a reaction catalyzed by the iron component). In the same way, zeolite-encapsulated ruthenium phthalocyanine (RuPc) and manganese porphyrin (Mn(TPP)) have been examined by Chan and Wilson [104] and found to mimic the methane oxygenase system. The authors claimed that methanol was obtained from methane, but at high temperature where the supported catalyst is not stable. Finally, Y-zeolite-encapsulated iron phthalocyanine and PdSalen complexes were shown to be catalysts for the selective hydrogenation of butadiene [71] and of hex-1-ene [60]. Specific zeolite effects have been reported, but further experiments are needed to rationalize them.

As a result of the encapsulation of the complexes and owing to their site isolation, a number of generalizations can be made from the analysis of the available data:

(1) turnover numbers increase when the catalyst is encapsulated (by comparison with the homogeneous solution catalysis, see Table 2),
(2) turnover numbers decrease with increased loading of the zeolite with complex. This points out problems associated with pore blockage,
(3) the dimensions and shape of the environment of the active sites control shape and regio-selectivity, as well as reactant diffusion,
(4) high yields (based on starting substrate) of oxygenated products (in biomimetic oxidations) are mostly obtained with pure and highly diluted entrapped complexes.

6. Conclusion

It appears from the reported work on biomimetic oxidations using clay-intercalated and zeolite-encapsulated catalysts that the idea of building into the mineral host the

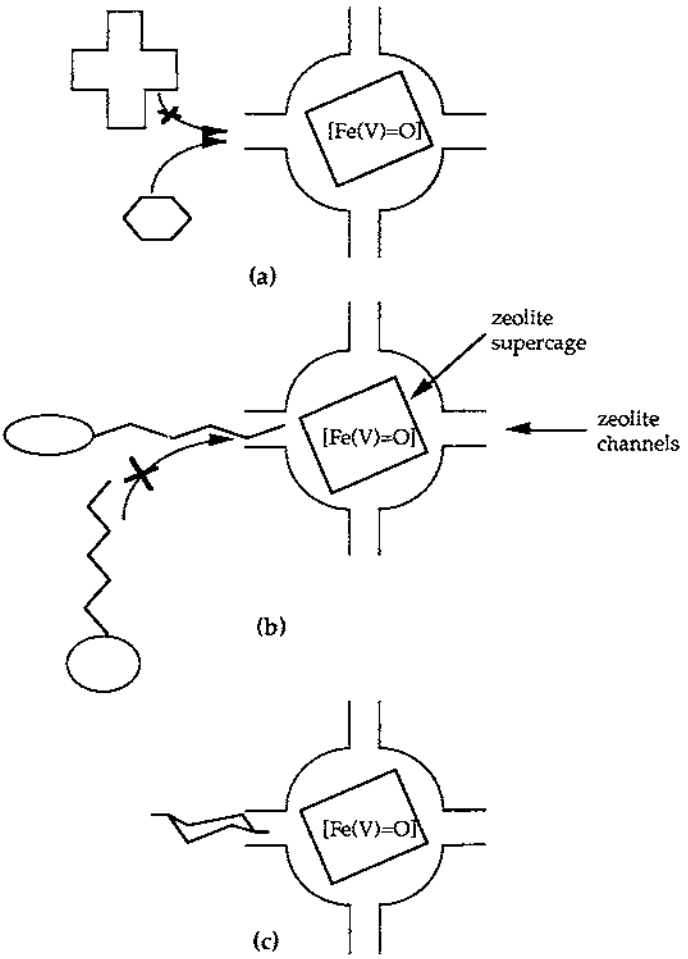

Fig. 17. Schematic representation of (a) substrate, (b) regio- and (c) stereoselectivities in zeolite cages containing the [Fe(V)=O]$^{+}$ oxo species (adapted from Ref. [8]).

ability to mimic certain biological processes is realistic. The zeolite framework and the clay layered structures, which have been compared to a protein, prevent entrapped metal complexes from dimerizing and degrading. The internal channels and cavities, by controlling the access and transport of substrate molecules to the zeolite cages and clay interlayer spacings, impose shape-, size- and stereo-selectivities in the same way as do channels created by the protein structure of an enzyme. In most cases, rates of reaction are extremely slow, and pore blockage leads to shutdown of the reactivity after a few catalytic cycles. These problems are serious, but they can easily be resolved, since many exciting advances are now being made in the design of new mineral hosts. The significant trends in molecular sieve science and technology, such as the synthesis of larger-pore zeolites and pillared clays having defined structures,

Table 2
Some examples of biomimetic oxidation of hydrocarbon by zeolite-encapsulated complexes

Catalyst	Oxygen donor	Substrate	Turnover number	Reference
FePc	PhIO	methylcyclohexane	1.1	[66]
FePc/Y (1%)[b]	PhIO	methylcyclohexane	5.6	[66]
FePc/X (2%)[b]	PhIO	methylcyclohexane	4.1	[66]
FePc/X (20%)[b]	PhIO	methylcyclohexane	0.5	[66]
FePc	tBuOOH	octane	25	[74]
FePc/Y (1/77)[c]	tBuOOH	octane	6000	[74]
MnSalen/Y (0.17%)[d]	PhIO	cyclohexene	60	[57]
Fe (TMP)	PhIO	cyclohexane	0.09	[91]
Fe(TMP)/Y (0.94%)[d]	PhIO	cyclohexane	0.16	[91]
Mn(TMP)/Y (6.6%)[d]	PhIO	cyclohexane	0.08	[91]

[a] It is not clear from all the reported studies if the turnover numbers are expressed per time unit or not.
[b] Percentage of cation exchanged by Fe(II).
[c] Number of encapsulated FePc per Y zeolite supercage.
[d] Metal loading; TMP: tetramethylporphyrin.

should act in favor of a more intense exploration of the research field of inorganic models.

Acknowledgments

Dr. J. Devynck, Dr. L. Gaillon and L. Roué from the Laboratoire d'Electrochimie et de Chimie Analytique (URA no. 216 du CNRS, Ecole Nationale Supérieure de Chimie de Paris), Dr. P. Battioni from the Laboratoire de Chimie et Biochimie Pharmacologiques et Toxicologiques (URA no. 400 du CNRS, Université René Descartes, Paris) and Professor K. J. Balkus, Jr. from the Department of Chemistry of the University of Texas at Dallas are gratefully acknowledged for their very helpful contribution.

References

[1] R.E. White and M.J. Coon, Ann. Rev. Biochem., 49 (1980) 315.
[2] I.C. Gunsalus and S.C. Sligar, Adv. Enzymol., 47 (1978) 1.
[3] D. Mansuy and P. Battioni, in J. Reedijk (ed.), Bioinorganic Catalysis, Marcel Dekker, New York, 1993, p. 395.
[4] A.E. Shilov, J. Molecular Catal., 47 (1988) 351.
[5] B.R. Cook, T.J. Reinert and K.S. Suslick, J. Am. Chem. Soc., 108 (1986) 7281.
[6] K. Suslik, B. Cook and M. Fox, J. Chem. Soc., Chem. Commun. (1980) 580.
[7] J.P. Collman, X. Zhang, V.J. Lee, U.S. Uffelman and J.I. Brauman, Science, 261 (1993) 1404, and references cited therein.
[8] N. Herron, J. Coord. Chem., 19 (1988) 25.
[9] N. Herron, Chemtech, (1989) 542.

[10] P.C.H. Mitchell, Chem. Ind. (1991) 308, and references cited therein.
[11] D. Mansuy, Coord. Chem. Rev., 125 (1993) 129.
[12] K.D. Karlin, Science, 261 (1993) 701.
[13] R. Parton, D. De Vos and P.A. Jacobs, in E.G. Derouane (ed.), Zeolite Microporous Solids: Synthesis, Structure, and Reactivity, Kluwer, Amsterdam, Netherlands, 1992, p. 555.
[14] H. Van Olphen, An Introduction to Clay Colloid Chemistry, Wiley, New York, 1977.
[15] G.W. Brindley and G. Brown (eds.), Crystal Structure of Clay Minerals and their X-ray Identification, Monograph 5, Mineral Society, London, 1980.
[16] S. Miyata, Clays Clay Miner., 23 (1975) 369.
[17] T.J. Pinnavaia, Science, 220 (1983) 365.
[18] J.M. Butruille and T.J. Pinnavaia, in I.E. Wachs (ed.), Characterization of Catalytic Materials, Butterworth-Heinemann, Boston, 1992, p. 149.
[19] D.W. Breck, Zeolite Molecular Sieves, Wiley, New York, 1974.
[20] R.M. Barrer, Hydrothermal Chemistry of Zeolites, Academic Press, New York, 1982.
[21] E.M. Falnigen, B. Lok, R.L. Patton and S.T. Wilson, Pure Appl. Chem., 58 (1986) 1351.
[22] J.V. Smith, Chem. Rev., 88 (1988) 142.
[23] G.A. Ozin, A. Kuperman and A. Stein, Angew. Chem. Int. Ed. Engl., 28 (1989) 359.
[24] S.L. Suib, Chem. Rev., 93 (1993) 803.
[25] M.E. Davis, Acc. Chem. Research, 26 (1993) 111.
[26] D.R. Kosiur, Clays and Clay Minerals, 25 (1977) 365..
[27] S.S. Cady and T.J. Pinnavaia, Inorg. Chem., 17 (1978) 1501.
[28] F. Bergaya and H. Van Damme, Geochim. Cosmochim. Acta, 46 (1982) 349.
[29] N. Hu and J.F. Rusling, Anal. Chem., 63 (1991) 2163.
[30] J.F. Rusling, M.F. Ahmadi and N. Hu, Langmuir, 8 (1992) 2455.
[31] H. Zhang and J.F. Rusling, Talanta, 40 (1993) 741.
[32] H. Kameyama, H. Suzuki and A. Amano, Chem. Lett. (1988) 117.
[33] L. Barloy, P. Battioni and D. Mansuy, J. Chem. Soc., Chem. Commun. (1990) 1365.
[34] K.A. Carrado and R.E. Winans, Chem. Mater., 2 (1990) 328.
[35] L. Barloy, J.P. Lallier, P. Battioni, D. Mansuy, Y. Piffard, M. Tournoux, J.B. Valim and W. Jones, New J. Chem., 16 (1992) 71.
[36] L. Gaillon, F. Bedioui, J. Devynck, P. Battioni, L. Barloy and D. Mansuy, J. Electroanal. Chem., 303 (1991) 283.
[37] K.A. Carrado, P. Thiyagarajan, R.E. Winans and R.E. Botto, Inorg. Chem., 30 (1991) 794.
[38] K.A. Carrado, J.E. Forman, R.E. Botto and R.E. Winans, Chem. Mater., 5 (1993) 472.
[39] M. Onaka, T. Shinoda, Y. Izomi and E. Nolen, Chem. Lett. (1993) 449.
[40] M. Onaka, T. Shinoda, Y. Izumi and E. Nolen, Tetrahedron Lett., 34 (1993) 2625.
[41] P. Laszlo and J. Luchetti, Chem. Lett. (1993) 449.
[42] M. E. Pèrez-Bernal, R. Ruano-Casero and T.J. Pinnavaia, Catal. Lett., 11 (1991) 55.
[43] M. Chibwe and T.J. Pinnavaia, J. Chem. Soc., Chem. Commun. (1993) 278.
[44] F. Bedioui, L. Gaillon, J. Devynck and P. Battioni, J. Electroanal. Chem., 347 (1993) 435.
[45] I.Y. Park, K. Kuroda and C. Kato, Chem. Lett. (1989) 2057.
[46] M.J. Hudson, W.J. Locke and P.C.H. Mitchell, Solid State Ionics, 61 (1993) 131.
[47] R.M. Kim, J.E. Pillion, D.A. Burwell, J.T. Groves and M.E. Thompson, Inorg. Chem., 32 (1993) 4509.
[48] P.R. Ortiz de Montenallo, Cytochrome P-450: Structure, Mechanism and Biochemistry, Plenum Press, New York, 1986.
[49] B. Meunier, Chem. Rev., 92 (1992) 1411.
[50] P.S. Dixit and K. Srinivasan, Inorg. Chem., 27 (1988) 4507.
[51] F. Bedioui, L. Gaillon, J. Devynck and P. Battioni, J. Mol. Catal., 78 (1993) L23.
[52] H. Pinochet and J. Devynck, Ann. Quim., 86 (1990) 35.
[53] L. Gaillon, Ph.D. Thesis, Université Pierre et Marie Curie, Paris VI (France), 1993.
[54] B. de Vismes, F. Bedioui, J. Devynck and C. Bied-Charreton, J. Electroanal. Chem., 187 (1985) 197.
[55] B. de Vismes, F. Bedioui, J. Devynck, M. Perrée-Fauvet and C. Bied-Charreton, N. J. Chim., 10 (1986) 81.

[56] N. Herron, Inorg. Chem., 25 (1986) 4714.
[57] C. Bowers and P.K. Dutta, J. Catal., 122 (1990) 271.
[58] L. Gaillon, N. Sajot, F. Bedioui, J. Devynck and K.J. Balkus Jr., J. Electroanal. Chem., 345 (1993) 157.
[59] K.J. Balkus Jr., A.A. Welch and B.E. Gnade, Zeolites, 10 (1990) 722.
[60] S. Kowalak, R.C. Weiss and K.J. Balkus Jr., J. Chem. Soc., Chem. Commun (1991) 57.
[61] B.V. Romanovsky, Proc. 8th Int. Congr. Catal., Verlag Chemie, Weinheim (1984) 657.
[62] G. Meyer, D. Wöhrle, M. Mohl and G. Schulz-Ekloff, Zeolites, 4 (1984) 30.
[63] H. Diegruber, P.J. Plath and G. Schulz-Ekloff, J. Mol. Catal., 24 (1984) 115.
[64] E.S. Shpiro, G.V. Antoshin, O.P. Tkachenko, S.V. Gudkov, B.V. Romanovsky and Kh.M. Minachev, Stud. Surf. Sci. Catal., 18 (1984) 31.
[65] A.N. Zakharov and B.V. Romanosky, J. Inclus. Phenom., 3 (1985) 389.
[66] N. Herron, G.D. Stucky and C.A. Tolman, J. Chem. Soc., Chem. Commun. (1986) 1521.
[67] C.A. Tolman and N. Herron, Catal. Today, 3 (1988) 235.
[68] Y.W. Chan and R.B. Wilson, Prep. Pap., ACS, Div. Fuel. Chem., 33 (1988) 453.
[69] G. Schulz-Ekloff, D. Wöhrle, V. Iliev, E. Ignatzek and A. Andreev, Stud. Surf. Sci. Catal., 46 (1989) 315.
[70] M. Tanaka, Y. Sakai, T. Tominga, A. Fukuoka, T. Kimura and M. Ichikawa, J. Radioanal. Nucl. Chem. Lett., 137 (1989) 287.
[71] T. Kimura, A. Fukuoka and M. Ichikawa, Catal. Lett., 4 (1990) 279.
[72] G. Schulz-Ekloff, D. Wöhrle and A. Andreev, Wissensch. Zeitschr. Leuna-Mersburg, 32 (1990) 649.
[73] K.J. Balkus Jr. and J.P. Ferraris, J. Phys. Chem., 94 (1990) 8019.
[74] R.F. Parton, L. Uytterhoeven and P.A. Jacobs, Stud. Surf. Sci. Catal., 59 (1991) 395.
[75] R.F. Parton, D.R.C. Huybrechts, Ph. Buskens and P.A. Jacobs, Stud. Surf. Sci. Catal., 65 (1991) 110.
[76] D.R.C. Huybrechts, R.F. Parton and P.A. Jacobs, Stud. Surf. Sci. Catal., 60 (1991) 225.
[77] R.F. Parton, D.R.C. Huybrechts, P. Buskens and P.A. Jacobs, Stud. Surf. Sci. Catal., 65 (1991) 47.
[78] M. Ichikawa, T. Kimura and A. Fukuoka, Stud. Surf. Sci. Catal., 60 (1991) 335.
[79] A.N. Zakharov, Mendeleev Commun. (1991) 80.
[80] Z. Jiang and Z. Xi, Fenzi Cuihua, 6 (1992) 467.
[81] K.J. Balkus Jr., A.A. Welch and B.E. Gnade, J. Inclus. Phenom. Molec. Recogn., 10 (1992) 141.
[82] J.P. Ferraris, K.J. Balkus Jr. and A. Schade, J. Inclus. Phenom. Molec. Recogn., 14 (1992) 163.
[83] B.V. Romanovsky and A.G. Gabrielov, J. Mol. Catal., 74 (1992) 293.
[84] M. Tanaka, Y. Minai, T. Watanabe and T. Tominaga, J. Radioanal. Nucl. Lett., 164 (1992) 255.
[85] E. Pács-Mozo, N. Gabriunas, F. Lucaccioni, D.D. Acosta, P. Patrono, A. La Ginestra, P. Ruis and B. Delmon, J. Phys. Chem., 97(1993) 12819.
[86] F. Bedioui, L. Roué, L. Gaillon, J. Devynck, S. L. Bell and K.J. Balkus Jr., Petrol Preprints, ACS, Div. Petrol Chem., 38 (1993) 529.
[87] A.G. Gabrielov, K.J. Balkus Jr., S.L. Bell, F. Bedioui and J. Devynck, Microp. Mater., 2 (1994) 119.
[88] K.J. Balkus Jr., A.G. Gabrielov, S.L. Bell, F. Bedioui, L. Roué and J. Devynck, Inorg. Chem., 33 (1994) 67.
[89] R.F. Parton, C.P. Bezoukhanova, J. Grobet, P.J. Grobet and P.A. Jacobs, Stud. Surf. Sci. Catal., in press.
[90] K.J. Balkus Jr., C.D. Hargis and S. Kowalak, ACS Symp. Ser., 499 (1992) 347.
[91] M. Nakamura, T. Tatsumi and H. Tominaga, Bull. Chem. Soc. Jpn., 63 (1990) 3342.
[92] D.R. Rolisson, Chem. Rev., 90 (1990) 867.
[93] A.J. Bard and T.E. Mallouk, in R.W. Murray (ed.), Molecular Design of Electrode Surfaces, Wiley, New York, 1992, p. 271.
[94] J.S. Krueger and T.E. Mallouk, in M. Gratzel and K. Kalyanasundaran (eds.), Kinetics and Catalysis in Microheterogeneous Systems, Dekker, New York, 1991, p. 461.
[95] F. Bedioui, E. De Boysson, J. Devynck and K.J. Balkus Jr., J. Electroanal. Chem., 315 (1991) 313.
[96] F. Bedioui, E. De Boysson, J. Devynck and K.J. Balkus Jr., J. Chem. Soc. Faraday Trans., 87 (1991) 3831.
[97] K. Mesfar, B. Carré, F. Bedioui and J. Devynck, J. Mater. Chem., 3 (1993) 873.

[98] F. Bedioui, L. Roué, E. Briot, J. Devynck, S.L. Bell and K.J. Balkus Jr., J. Electroanal. Chem., 337 (1994) 19 (and references cited therein).
[99] B.R. Shaw, K.E. Creasy, C.J. Lanczycki, J.A. Sargeant and M. Tirhado, J. Electrochem. Soc., 135 (1988) 869.
[100] K.B. Yoon, Chem. Rev., 93 (1993) 321, and references cited therein.
[101] F. Bedioui, L. Roué, J. Devynck and K.J. Balkus Jr., J. Electrochem Soc., 141 (1994) 3049.
[102] K. Mizuno, S. Imamura and J.H. Lunsford, Inorg. Chem., 23 (1984) 3510.
[103] R.A. Schoonheydt and J. Pelgrins, J. Chem. Soc., Dalton Trans. (1981) 914.
[104] Y.W. Chan and R.B. Wilson, ACS Prepr., Div. Petrol. Chem., 33 (1988) 271.